**Atmospheric
Chemistry
and Physics
Discussions**

Sensitivity analyses of OH missing sinks over Tokyo metropolitan area in the summer of 2007

S. Chatani[1,*]**, N. Shimo**[1]**, S. Matsunaga**[1]**, Y. Kajii**[2]**, S. Kato**[2]**, Y. Nakashima**[2]**,
K. Miyazaki**[2]**, K. Ishii**[3]**, and H. Ueno**[3]

[1]Japan Petroleum Energy Center, Tokyo, Japan
[2]Tokyo Metropolitan University, Tokyo, Japan
[3]Tokyo Metropolitan Research Institute for Environmental Protection, Tokyo, Japan
[*]Contracted researcher from Toyota Central R&D Labs., Inc., Aichi, Japan

Correspondence to: S. Chatani (schatani@mosk.tytlabs.co.jp)

ACPD

9, 18479–18509, 2009

Sensitivity analyses of OH missing sinks over Tokyo

S. Chatani et al.

Title Page

Abstract	Introduction
Conclusions	References
Tables	Figures

Back | Close

Full Screen / Esc

Printer-friendly Version

Interactive Discussion

Sensitivity analyses of OH missing sinks over Tokyo

S. Chatani et al.

Abstract

OH reactivity is one of key indicators which reflect impacts of photochemical reactions in the atmosphere. An observation campaign has been conducted in the summer of 2007 at the heart of Tokyo metropolitan area to measure OH reactivity. The total OH reactivity measured directly by the laser-induced pump and probe technique was higher than the sum of the OH reactivity calculated from concentrations and reaction rate coefficients of individual species measured in this campaign. And then, three-dimensional air quality simulation has been conducted to evaluate the simulation performance on the total OH reactivity including "missing sinks", which correspond to the difference between the measured and calculated total OH reactivity. The simulated OH reactivity is significantly underestimated because the OH reactivity of volatile organic compounds (VOCs) and missing sinks are underestimated. When scaling factors are applied to input emissions and boundary concentrations, a good agreement is observed between the simulated and measured concentrations of VOCs. However, the simulated OH reactivity of missing sinks is still underestimated. Therefore, impacts of unidentified missing sinks are investigated through sensitivity analyses. In the cases that unknown secondary products are assumed to account for unidentified missing sinks, they tend to suppress formation of secondary aerosol components and enhance formation of ozone. In the cases that unidentified primary emitted species are assumed to account for unidentified missing sinks, a variety of impacts may be observed, which could serve as precursors of secondary organic aerosols (SOA) and significantly increase SOA formation. Missing sinks are considered to play an important role in the atmosphere over Tokyo metropolitan area.

1 Introduction

Air quality in Japan has been improved, however, some problems are still remained unresolved. NO_2 concentrations at some roadside monitoring stations located in urban

area exceed the Environmental Quality Standards (EQSs) in Japan. O_3 concentrations are gradually increasing and the EQSs for photochemical oxidants have not been satisfied at almost all monitoring stations in whole Japan (Ministry of the Environment, 2008). In addition, $PM_{2.5}$ concentrations in Japanese urban areas are likely higher than
5 the air quality standards implemented in the United States and Europe.

Most of NO_2, O_3 and $PM_{2.5}$ are secondarily produced through photochemical reactions in the atmosphere. Their concentrations nonlinearly respond to emissions of various precursors (Meng et al., 1997). In order to consider how to reduce concentrations of secondary products, it is necessary to perform simulations using a three-
10 dimensional air quality model in which complex photochemical reactions are involved. However, it is inevitably important to determine the reliability of the simulation results, that is, whether simulated responses of secondary products to precursor emissions are reliable. Observation data of critical pollutants (e.g. NO_2 and O_3) are mainly used for validation, but more thorough validation is desirable.
15 Though progresses in measuring instruments and techniques have realized identification of various trace species, many atmospheric trace species have remained unidentified. Their importance on photochemical reactions needs to be evaluated. Total OH reactivity is one of key indicators which reflect the impacts of identified and unidentified species on photochemical reactions and secondary products. It is also
20 useful as an indicator to validate the three-dimensional air quality simulations in terms of complex photochemical reactions.

A technique to directly measure total OH reactivity has been developed by Sadanaga et al. (2004). Yoshino et al. (2006) used this technique to perform direct measurement of total OH reactivity at Hachioji, Japan, which is located about 30 km west of the heart
25 of Tokyo metropolitan area. As well as total OH reactivity, they measured concentrations of various species and calculated OH reactivity from concentrations of measured species and their known reaction rate coefficients with OH. They found that the directly measured total OH reactivity was always higher than the sum of the OH reactivity of measured individual species. The difference between the measured and calculated

**Sensitivity analyses
of OH missing sinks
over Tokyo**

S. Chatani et al.

total OH reactivity is called "missing sinks", which may affect photochemical reactions and secondary product formation in the atmosphere.

In order to further investigate the impacts of missing sinks within the metropolitan area, an observation campaign has been conducted in the summer of 2007 at the heart of Tokyo metropolitan area. Total OH reactivity and concentrations of various species were measured in this campaign. And then, we executed the three-dimensional air quality model and compared the simulation results with the observation results. The air quality models treat photochemical reactions in aggregated forms as in CB4 (Gery et al., 1989) and SAPRC99 (Carter, 2000) chemical mechanisms. Missing sinks should be part of some aggregated species groups defined in the chemical mechanisms. To validate the simulations in terms of photochemical reactions, we have examined whether the simulation can reproduce the measured total OH reactivity including missing sinks. In addition, we have conducted sensitivity analyses to investigate the impacts of missing sinks on photochemical reactions and secondary products.

Recently, OH reactivity has been used to validate three-dimensional air quality simulations. Steiner et al. (2008) and Stroud et al. (2008) investigated OH reactivity in central California and Canada, respectively. They calculated OH reactivity from measured and simulated concentrations of various species, and compared them. However, measured total OH reactivity and missing sinks were not used directly in these papers. In this study, simulated OH reactivity is compared with the directly measured OH reactivity including missing sinks. In addition, impacts of missing sinks are investigated through sensitivity analyses.

An overview of the three-dimensional air quality simulations are described in Sect. 2. A brief description of the observation campaign is provided in Sect. 3. Performance of the three-dimensional air quality simulation for OH reactivity is described in Sect. 4. Results of sensitivity analyses of missing sinks are described in Sect. 5. And the outcomes are summarized in Sect. 6.

Sensitivity analyses of OH missing sinks over Tokyo

S. Chatani et al.

⏮   ⏭

◀   ▶

Back   Close

Full Screen / Esc

Printer-friendly Version

Interactive Discussion

Sensitivity analyses of OH missing sinks over Tokyo

S. Chatani et al.

2 Overview of three-dimensional air quality simulations

We have developed a three-dimensional air quality simulation framework which consists of the Weather Research and Forecasting (WRF) model for meteorology, the Community Multi-scale Air Quality (CMAQ) modeling system for pollutant concentrations, and emission inventory models. The below describes how to perform simulations.

2.1 Target domains

Target domains of the three-dimensional air quality simulations are shown in Fig. 1. Three nested domains are used in the simulation: East Asia, Japan, and Kanto (including Tokyo metropolitan area). Horizontal coordinate system is based on Lambert conformal conic projection and the reference latitude and longitude coordinates are given as 36° N, 128° E for East Asia domain, and 38.1° N, 136.9° E for Japan and Kanto domains. Domain dimensions for WRF are 5832×4248 km for East Asia, 2000×2000 km for Japan and 336×384 km for Kanto region, respectively, while for CMAQ, slightly smaller domains are given. Vertical coordinate system is based on the sigma-P coordinate system and the top pressure is 100 hPa. The number of vertical layers of East Asia, Japan and Kanto domains for WRF is 31, 34 and 34, respectively, while for CMAQ, the number is merged into 20, 23 and 23, respectively. Approximate height of bottom layer is 57 m in East Asia, and 16 m in Japan and Kanto domains. Grid dimensions are 36×36 km for East Asia, 16×16 km for Japan and 4×4 km for Kanto domain, respectively. In WRF simulation, calculations of East Asia domain are done separately, while calculations of Japan and Kanto domains are done simultaneously using a two-way nesting approach. In CMAQ simulation, calculations of East Asia, Japan and Kanto domains are done consecutively using a one-way nesting approach.

2.2 Input emission data

Motor vehicle emission inventory model developed under Japan AuTo-Oil Program (JATOP) (Japan Petroleum Energy Center, 2009) is used to calculate motor vehicle emission inventories in Japan. The model can estimate hourly running, start and evaporative emissions. Georeference-Based Emission Activity Modeling System (GBEAMS) (Nansai et al., 2004) is used to calculate hourly emissions from anthropogenic sources except for vehicles in Japan. Regional Emission inventory in ASia (REAS) ver. 1.11 (Ohara et al., 2007) is used for preparing anthropogenic emissions in East Asia domain. Model of Emissions of Gases and Aerosols from Nature (MEGAN) v2.04 (Guenther et al., 2006) is used to estimate biogenic VOC emissions.

2.3 Meteorology and air quality models

WRF-ARW ver. 2.2.1 (Skamarock et al., 2005) is used to prepare meteorological fields. NCEP Final Analysis data are used to provide initial and boundary conditions, and to perform grid nudging. CMAQ ver. 4.6 (Byun et al., 2006) is used to simulate pollutant concentrations in the atmosphere. SAPRC99 (Carter, 2000) is chosen for the chemical mechanism. Table 1 shows relationships between the species measured in the observation campaign and the SAPRC99 species which react with OH. Measured species are allocated to one of the SAPRC99 species. These SAPRC99 species are further merged into species groups – abbreviated as AVOC, BVOC and OVOC – as shown in Table 1. However, no measured species are allocated to the SAPRC99 species listed in the "missing sinks" group in Table 1, which are treated as missing sinks in this paper.

3 Overview of the observation campaign

Overview of the observation campaign is described in this section. And the details have been published by Nakashima et al. (2009).

An observation campaign has been conducted from 21–27 August 2007 in Koto-Ku, Tokyo, which is close to the heart of Tokyo metropolitan area as shown in Fig. 1. Data obtained during daytime of 21, 22, 26 and 27 August are used for the analysis of this paper. Ambient air is introduced into the reaction flow tube. A laser beam is used to irradiate the incident window of the reaction tube and OH radicals are artificially generated. Changes in OH concentrations are detected by the laser-induced pump and probe technique. Total OH reactivity is represented by the decay rate of OH. In addition, measurements have been conducted on concentrations of critical species (NO_2, NO, O_3, CO and SO_2), various individual non-methane hydrocarbons (NMHCs) and oxygenated volatile organic compounds (OVOCs). All of measured species and corresponding SAPRC99 species are listed in Table 1.

Figure 2 shows the directly measured and calculated total OH reactivity, of which calculations are obtained from concentrations and reaction rate coefficients of the measured species on August 21, as an example. Existing databases (Atkinson, 2004, 2007; Atkinson et al., 1997; Calvert et al., 2000; Sander et al., 2002) are used for reaction rate coefficients except for the reaction rate coefficient of NO_2+OH, for which the measured values are used. The directly measured values of total OH reactivity are mostly higher than the sum of the calculated OH reactivity. It implies the existence of missing sinks in the atmosphere over Tokyo metropolitan area.

Figure 3 shows contribution of species groups to the directly measured OH reactivity which is averaged over the target period. NO_2 and AVOC are major contributors, but fraction of the missing sinks is larger than that of NO_2 and AVOC. Therefore, it implies that missing sinks are playing an important role in photochemical reactions and secondary product formation in the atmosphere over Tokyo metropolitan area.

4   Results of the simulation

The three-dimensional air quality simulation was executed for the period including daytime of 21, 22, 26 and 27 August 2007. Figure 4 shows ratios of the simulated con-

Sensitivity analyses of OH missing sinks over Tokyo

S. Chatani et al.

centrations to the measured concentrations of SAPRC99 species which is averaged over the target period. Ratios of almost all of SAPRC99 VOC species are significantly lower than 1.0. The most probable reason for the underestimation is due to the emission inventory. Solvent use is recognized as a major contributing source to total VOC emissions in Japan (Kannari et al., 2007), however, the emission estimates have large uncertainty. Their special and temporal distribution is also not well known. Obviously, more works are required to improve the emission inventory estimation, especially for VOC emissions. Another possible reason for the underestimation is meteorological conditions during the observation campaign. Wind direction in daytime is mostly southerly during the target period. The observation site is located in a few kilometres north of Tokyo Bay. There are few major pollutant sources in the south of the measurement site. It is well known that pollutant distribution over the coastal area of Tokyo Bay is affected by sea-land breeze and heat-island effect (Yoshikado, 1992). It is considered the simulation may have difficulty in reproducing detailed wind flow patterns caused by these factors.

Here, we assume a situation where the challenges in simulation stated above are resolved. Scaling factors for each SAPRC99 species are uniformly applied to input emissions and boundary concentrations. Scaling factors are defined by inverse numbers of the ratios shown in Fig. 4. This procedure is repeated twice to bring the simulated concentrations closer to the measured concentrations. TRP1 is excluded from this procedure, because it is originated from biogenic sources, and uniform scaling factors defined in the metropolitan area may cause a significant overestimation in rural areas. Ratios of the simulated concentrations to the measured concentrations obtained by application of scaling factors are also shown in Fig. 4. Ratios of NO, O_3 and HCHO are not close to 1.0 because they are largely affected by secondary products. There are difficulties in achieving an agreement between measured and calculated concentrations for these species. Except for these species, the procedure makes the ratios closer to 1.0.

Figure 5 shows time series of the measured and simulated hourly concentrations of

species groups before and after application of scaling factors. The absolute level and hourly variations of concentrations of critical species are reproduced well. However, the simulated concentrations of AVOC, BVOC and OVOC are significantly underestimated before application of scaling factors. Application of scaling factors makes their concentrations closer to the measured ones. Hourly variations of AVOC and OVOC are also reproduced well. Figure 6 shows time series of the measured and simulated hourly total OH reactivity before and after application of scaling factors. Simulated total OH reactivity is calculated from the simulated concentrations of SAPRC99 species and their reaction rate coefficients with OH defined in SAPRC99. The measured total OH reactivity tends to be high in the morning and evening, while low around noon. Such hourly variations in total OH reactivity are reproduced in the simulations; however, the values are underestimated before application of scaling factors. Application of scaling factors also makes the simulated OH reactivity closer to the measured one.

Figure 7 shows the measured and simulated OH reactivity of species groups which is averaged over the target period before and after application of scaling factors. Simulated OH reactivity of critical species shows a good agreement with the measurements. However, the simulated OH reactivity of AVOC, BVOC and OVOC is significantly underestimated before application of scaling factors. The underestimation of these species groups is considered as a major cause of underestimated total OH reactivity. Application of scaling factors makes the simulated total OH reactivity closer to the measured one. However, further considerations are required on the contribution of the species groups to total OH reactivity.

As shown in Fig. 4, the simulated concentrations of each species included in AVOC show a good agreement with the measured ones, which leads to an expectation that the simulated OH reactivity of AVOC will achieve a good agreement with the measured ones. However, the fact is that the simulated OH reactivity of AVOC is higher than the measured one. It indicates that reaction rate coefficients of AVOC with OH in SAPRC99 are higher than those of measured AVOC species. One possible reason is that SAPRC99 assumes the existence of species which are never measured in the

observation campaign and having higher reaction rate coefficients with OH than those of measured AVOC species. If such species really exist in the atmosphere, they may be included in the missing sinks in measured total OH reactivity. In addition, not only the simulated OH reactivity but also simulated concentrations of AVOC should be higher than the measured values. Impacts of the missing sinks for which AVOC might account will be discussed in the next section. Another possible reason is that SAPRC99 is not suitable for simulating the atmosphere over Tokyo metropolitan area. A lumping approach in which VOC species are combined into groups is used in SAPRC99, which might result in the differences in measured and calculated OH reactivity of VOC groups over Tokyo metropolitan area. The simulated OH reactivity of OVOC is higher than the measured OH reactivity, simply because HCHO is still overestimated after application of scaling factors. Coincidence may be achieved between measured and simulated OH reactivity if simulated concentrations of HCHO could be agreed with the measured ones. The simulated OH reactivity of missing sinks ($5.3\,\mathrm{s}^{-1}$) is lower than the measured one ($8.5\,\mathrm{s}^{-1}$). The simulation can explain about 60% of the measured OH reactivity of missing sinks by species groups treated in SAPRC99, however, remaining 40% cannot be explained. Impacts of remaining unexplained missing sinks (about $3.0\,\mathrm{s}^{-1}$) will be discussed through sensitivity analyses in the next section.

5   Sensitivity analyses of OH missing sinks

As shown in the previous section, the simulated OH reactivity of missing sinks is about $3.0\,\mathrm{s}^{-1}$ lower than the measured one. Possible candidates for unexplained missing sinks are unknown secondary products and unidentified primary emitted species. Sensitivity analyses are conducted to investigate their impacts on photochemical reactions and secondary product formation in the atmosphere. The simulation in which scaling factors are applied to input emissions and boundary concentrations (described in the previous section) is used as the base case in the sensitivity analyses.

Sensitivity analyses of OH missing sinks over Tokyo

S. Chatani et al.

Full Screen / Esc

Printer-friendly Version

Interactive Discussion

5.1 Impacts of unknown secondary products

It is impossible to estimate impacts of unknown secondary products because their reaction path and rate coefficients are also unknown. Therefore, we assumed that unknown secondary products have similar characteristics to the known secondary products. Figure 8 shows contribution of SAPRC99 species to the simulated OH reactivity of missing sinks which is averaged over the target period in the base case. RCHO represents a group of aldehydes with three or more carbons, DCB1 represents a group of reactive aromatic fragmentation products that do not undergo significant photodecomposition to radicals, and PROD2 represents a group of ketones and other non-aldehyde oxygenated products which react with OH radicals faster than 5×10^{-12} cm^3 molecuule^{-2} s^{-1} (Carter, 2000). Contribution of these groups to the simulated OH reactivity of missing sinks is 30% for RCHO, 10% for DCB1 and 8% for PROD2, respectively. They are major secondary products in the simulation, so that their impacts are investigated here. In order to increase their concentrations in sensitivity analyses, factors are multiplied to the individual yield of the groups (RCHO, DCB1 and PROD2) in SAPRC99 reactions, and then simulations are conducted for the three cases: chg-RCHO, chg-DCB1 and chg-PROD2. Multiplied factors to the yields for RCHO, DCB1 and PROD2 to add $3.0\,\mathrm{s}^{-1}$ to their OH reactivity are 4.6/1.6, 3.6/0.6 and 3.4/0.4, respectively.

Figure 9 shows the simulated OH reactivity of the species groups which is averaged over the target period for the base, chg-RCHO, chg-DCB1 and chg-PROD2 cases. The OH reactivity is expected to increase by $3.0\,\mathrm{s}^{-1}$, however, the fact is that the OH reactivity increases by more than $3.0\,\mathrm{s}^{-1}$ because increased RCHO, DCB1 and PROD2 form species which react with OH in subsequent reactions. Figure 10 shows incremental ratios of concentrations of NO_2, O_3, ambient OH and secondary aerosol components including SO_4^{2-}, NO_3^-, NH_4^+, anthropogenic secondary organic aerosol (ASOA) and biogenic SOA (BSOA) in the chg-RCHO, chg-DCB1 and chg-PROD2 cases compared to those in the base case which are averaged over the target period. The ambient OH

Title Page

Abstract | Introduction

Conclusions | References

Tables | Figures

◄◄ | ►►

◄ | ►

Back | Close

Full Screen / Esc

Printer-friendly Version

Interactive Discussion

decreases in all cases because additional OH is consumed by the increased RCHO, DCB1 and PROD2. As a result, oxidation of the precursors by OH is suppressed, and the decrease is observed in SO_4^{2-}, NO_3^- ASOA and BSOA, which are major oxidized products. NH_4^+ also decreases because of decreased SO_4^{2-} and NO_3^-, which are anions coupling mainly with NH_4^+. Although O_3 increases slightly, incremental ratios differ among the three cases.

Based on the results described above, missing sinks are considered to suppress formation of secondary aerosol components and enhance formation of ozone in the cases that unknown secondary components may account for the missing sinks which have similar characteristics to RCHO, DCB1 and PROD2.

5.2   Impacts of unidentified primary emitted species

Figure 11 shows contribution of SAPRC99 species to the simulated OH reactivity of AVOC which is averaged over the target period in the base case. Contribution of ALK5, OLE2 and ARO2 to the simulated OH reactivity of AVOC is 4%, 16% and 18%, respectively. They are aggregated species groups which have the highest reaction rate coefficients with OH among alkanes, olefins and aromatic compounds in SAPRC99. In the previous section, reaction rate coefficients of SAPRC99 AVOC species are higher than those of measured ones. If missing sinks which correspond to AVOC exist in the atmosphere, they are likely to have higher reaction rate coefficients and account for ALK5, OLE2 and ARO2. Therefore, factors are multiplied to input emissions and boundary concentrations of ALK5, OLE2 and ARO2 individually, and then the simulation is conducted for these three cases: chg-ALK5, chg-OLE2 and chg-ARO2. Multiplied factors of ALK5, OLE2 and ARO2 to add $3.0\,s^{-1}$ to their OH reactivity are 3.3/0.3, 4.2/1.2 and 4.3/1.3, respectively.

Figure 12 shows the simulated total OH reactivity of the species groups which is averaged over the target period in the base, chg-ALK5, chg-OLE2 and chg-ARO2 cases. The OH reactivity of AVOC increased by about $3.0\,s^{-1}$ in the chg-OLE2 and chg-ARO2

cases, while by more than $3.0\,\mathrm{s}^{-1}$ in the chg-ALK5 case. Possible reasons will be discussed later. The OH reactivity of OVOC and missing sinks slightly increases in all cases due to formation of secondary products from increased AVOC, and a resulting increase in the total OH reactivity is more than $3.0\,\mathrm{s}^{-1}$. Figure 13 shows incremental ratios of concentrations of NO_2, O_3 and secondary aerosol components in the chg-ALK5, chg-OLE2 and chg-ARO2 cases compared to those in the base case which is averaged over the target period. Signs and magnitudes of incremental ratios have a wider variety than cases for unknown secondary products. The ambient OH decreases in the chg-ALK5 case due to increased ALK5. As a result, available ambient OH for the reaction with ALK5 decreases, and then the OH reactivity of AVOC increases by more than $3.0\,\mathrm{s}^{-1}$ in the chg-ALK5 case. On the other hand, ambient OH slightly increases in the chg-OLE2 and chg-ARO2 cases. Products from photochemical reactions of OLE2 and ARO2 seem to contribute to the increase in ambient OH. ASOA concentrations increase significantly in the chg-ALK5 and chg-ARO2 cases because ALK5 and ARO2 are precursors of ASOA in SAPRC99. SOA formation is enhanced when organics mass concentrations in particle phase are high (Odum et al., 1996; Schell et al., 2001). Therefore, BSOA also increases in both cases, while no increase is observed in precursors of BSOA. O_3 increases slightly, however, the ratios vary among the three cases.

Based on the results described above, it can be said that the impacts of missing sinks are diversified in the cases that missing sinks are unidentified primary emitted species. Some species suppress, while others enhance the oxidation by OH. Some species could increase SOA formation. All of unidentified primary emitted species increase O_3 formation. In general, a lot of three-dimensional air quality simulations are facing problems of significant underestimation of organic aerosols (Volkamer et al., 2006). Presence of unidentified primary emitted species which are neglected in the simulation but play an important role as ASOA precursors in the atmosphere may be one of the reasons for underestimated organic aerosols.

Full Screen / Esc

Printer-friendly Version

Interactive Discussion

6 Summary

The three-dimensional air quality simulations are applied to the observation campaign which has been conducted in the summer of 2007, during which total OH reactivity and concentrations of various species were measured at the heart of Tokyo metropolitan area. The simulated total OH reactivity is significantly underestimated because of the underestimation of the simulated OH reactivity of AVOC, BVOC, OVOC and missing sinks. Emission inventory data is required to be improved. However, the simulation performance at different places in different seasons is not known. More measurement data in different conditions are needed to be collected to contribute to a thorough improvement of the emission inventory.

After application of scaling factors to input emissions and boundary concentrations, a good agreement is obtained between the simulated concentrations of most species groups and the measured concentrations. However, the simulated OH reactivity of missing sinks is still underestimated. This result implies that simulations are not accurate enough in terms of photochemical reactions even if concentrations of major species are simulated well. Based on the results of sensitivity analyses, unidentified missing sinks could suppress formation of secondary aerosol components and enhance formation of O_3, while could increase SOA production significantly if SOA precursors account for the missing sinks.

The range of incremental ratios of concentrations in sensitivity analyses can be regarded as one of potential uncertainties in the three-dimensional air quality simulations in terms of photochemical reactions. Identifying the missing sinks and revealing their photochemical reaction path and rate coefficients are essential to reduce the uncertainties. Advances in measurement instruments and techniques will be required to identify the missing sinks.

References

Atkinson, R.: Gas-phase tropospheric chemistry of organic compounds, J. Phys. Chem. Ref. Data, Monograph, 2, 1–216, 1994.

Atkinson, R.: Gas-phase tropospheric chemistry of volatile organic compounds, 1. Alkanes and alkenes, J. Phys. Chem. Ref. Data, 26, 215–290, 1997.

Atkinson, R., Baulch, D. L., Cox, R. A., Hampson, R. F., Kerr, J. A., Rossi, M. J., and Troe, J.: Evaluated kinetic and photochemical data for atmospheric chemistry: Supplement VI – IUPAC subcommittee on gas kinetic data evaluation for atmospheric chemistry, J. Phys. Chem. Ref. Data, 26, 1329–1499, 1997.

Byun, D. and Schere, K. L.: Review of the governing equations, computational algorithms, and other components of the Models-3 Community Multiscale Air Quality (CMAQ) modeling system, Appl. Mech. Rev., 59, 51–77, 2006.

Calvert, J. G., Derwent, R. G., Orlando, J. J., Tyndall, G. S., and Wallington, T. J.: Mechanisms of Atmospheric Oxidation of the Alkanes, Oxford University Press, New York, USA, 1008 pp., 2008.

Carter, W. P. L.: Implementation of the SAPRC-99 chemical mechanism into the models-3 framework, Report to the United States Environmental Protection Agency, 2000.

Gery, M. W., Whitten, G. Z., Killus, J. P., and Dodge, M. C.: A photochemical kinetics mechanism for urban and regional scale computer modelling, J. Geophys. Res., 94, 12 925–12 956, 1989

Guenther, A., Karl, T., Harley, P., Wiedinmyer, C., Palmer, P. I., and Geron, C.: Estimates of global terrestrial isoprene emissions using MEGAN (Model of Emissions of Gases and Aerosols from Nature), Atmos. Chem. Phys., 6, 3181–3210, 2006, http://www.atmos-chem-phys.net/6/3181/2006/.

Japan Petroleum Energy Center: http://www.pecj.or.jp/english/jcap/jatop/index_jatop.html, 2009.

Kannari, A., Tonooka, Y., Baba, T., and Murano, K.: Development of multiple-species 1 km×1 km resolution hourly basis emissions inventory for Japan, Atmos. Environ., 41, 3428–3439, 2007.

Meng, Z., Dabdub, D., and Seinfeld, J. H.: Chemical coupling between atmospheric ozone and particulate matter, Science, 277, 116–119, 1997.

Ministry of the Environment: http://www.env.go.jp/air/osen/index.html, 2008 (in Japanese).

Nakashima, Y., Matsuda, H., Ide, S., Miyazaki, K., Yamazaki, K., Okazaki, H., Osada, T., Tajima, Y., Suthawaree, J., Kato, S., Shimo, N., Matsunaga, S., Apel, E., Greenberg, J., Guenther, A., Ueno, H., Sasaki, H., Hoshi, J., Yoshino, A., Yokota, H., Ishii, K., and Kajii, Y.: Diagnosis of urban air quality by measurement of total OH reactivity II: Comprehensive observations in the urban of Tokyo, J. Jpn. Soc. Atmos. Environ., 44, 33–41, 2009 (in Japanese).

Nansai, K., Suzuki, N., Tanabe, K., Kobayashi, S., and Moriguchi, Y.: Design of Georeference-Based Emission Activity Modeling System (G-BEAMS) for Japanese emission inventory management, Proceedings of the 13th International Emission Inventory Conference in Clearwater, Florida, United States of America, 7–10 June 2004.

Odum, J. R., Hoffmann, T., Bowman, F., Collins, D., Flagan, R. C., and Seinfeld, J. H.: Gas/particle partitioning and secondary organic aerosol yields, Environ. Sci. Technol., 30, 2580–2585, 1996

Ohara, T., Akimoto, H., Kurokawa, J., Horii, N., Yamaji, K., Yan, X., and Hayasaka, T.: An Asian emission inventory of anthropogenic emission sources for the period 1980–2020, Atmos. Chem. Phys., 7, 4419–4444, 2007,
http://www.atmos-chem-phys.net/7/4419/2007/.

Sadanaga, Y., Yoshino, A., Watanabe, K., Yoshioka, A., Wakazono, Y., Kanaya, Y., and Kajii, Y.: Development of a measurement system of OH reactivity in the atmosphere by using a laser-induced pump and probe technique, Rev. Sci. Instrum., 75, 2648–2655, 2004.

Sander, S. P., Friedl, R. R., Golden, D. M., Kurylo, M. J., Huie, R. E., Orkin, V. L., Moortgat, G. K., Ravishankara, A. R., Kolb, C. E., Molina, M. J., and Finlayson-Pitts, B. J.: Chemical kinetics and photochemical data for use in atmospheric studies, Evaluation No. 14, JPL Publication 02-25, 2003.

Schell, B., Ackermann, I. J., Hass, H., Binkowski, F. S., and Ebel, A.: Modeling the formation of secondary organic aerosol within a comprehensive air quality model system, J. Geophys. Res., 106, 28 275–28 293, 2001.

Skamarock, W. C., Klemp, J. B., Dudhia, J., Gill, D. O., Barker, D. M., Wang, W., and Powers, J. G.: A description of the advanced research WRF version 2, NCAR Technical Note, NCAR/TN–468+STR, 2005.

Steiner, A. L., Cohen, R. C., Harley, R. A., Tonse, S., Millet, D. B., Schade, G. W., and Goldstein, A. H.: VOC reactivity in central California: comparing an air quality model to ground-based measurements, Atmos. Chem. Phys., 8, 351–368, 2008,

Title Page

Abstract | Introduction

Conclusions | References

Tables | Figures

◄◄ | ►►

◄ | ►

Back | Close

Full Screen / Esc

Printer-friendly Version

Interactive Discussion

http://www.atmos-chem-phys.net/8/351/2008/.

Stroud, C. A., Morneau, G., Makar, P. A., Moran, M. D., Gong, W., Pabla, B., Zhang, J., Bouchet, V. S., Fox, D., Venkatesh, S., Wang, D., and Dann, T.: OH-reactivity of volatile organic compounds at urban and rural sites across Canada: Evaluation of air quality model predictions using speciated VOC measurements, Atmos. Environ., 42, 7746–7756, 2008

Volkamer, R., Jimenez, J. L., San Martini, F., Dzepina, K., Zhang, Q., Salcedo, D., Molina, L. T., Worsnop, D. R., and Molina, M. J.: Secondary organic aerosol formation from anthropogenic air pollution: Rapid and higher than expected, Geophys. Res. Lett., 33, L17811, doi:10.1029/2006GL026899, 2006.

Yoshikado, H.: Numerical study of the daytime urban effect and its interaction with the sea breeze, J. Appl. Meteorol., 31, 1146–1164, 1992

Yoshino, A., Sadanaga, Y., Watanabe, K., Kato, S., Miyakawa, Y., Matsumoto, J., and Kajii, K.: Measurement of total OH reactivity by laser-induced pump and probe technique – comprehensive observations in the urban atmosphere of Tokyo, Atmos. Environ., 40, 7869–7881, 2006.

Sensitivity analyses of OH missing sinks over Tokyo

S. Chatani et al.

Title Page

Abstract | Introduction

Conclusions | References

Tables | Figures

◀◀ | ▶▶

◀ | ▶

Back | Close

Full Screen / Esc

Printer-friendly Version

Interactive Discussion

Table 1. Relationships among species group, SAPRC99 species and individual species measured in the observation campaign in this study.

Species group	SAPRC99 species	Measured species
NO_2	NO2	NO_2
NO	NO	NO
O_3	O3	O_3
CO	CO	CO
SO_2	SO2	SO_2
AVOC	ALK1	ethane
	ALK2	acetylene, propane
	ALK3	isobutane, *n*-butane, 2,2-dimethylbutane
	ALK4	2,3-dimethylbutane, isopentane, *n*-pentane, cyclopentane, 2-methylpentane, 3-methylpentane, *n*-hexane, methylcyclopentane, 2,4-dimethylpentane, 2,2,4-trimethylpentane
	ALK5	cyclohexane, 2-methylhexane, 2,3-dimethylpentane, 3-methylhexane, *n*-heptane, methylcyclohexane, 2,3,4-trimethylpentane, 2-methylheptane, 3-methylheptane, *n*-octane, *n*-nonane
	ETHENE	Ethene
	OLE1	propylene, 1-butene, 3-methyl-1-butene, 1-pentene, 4-methyl-1-pentene
	OLE2	butadiene, *trans*-2-butene, *cis*-2-butene, *trans*-2-pentene, *cis*-2-pentene, 2-methyl-2-butene, cyclopentene, 2-methyl-1-pentene, *trans*-2-hexene, *cis*-2-hexene, styrene
	ARO1	benzene, toluene, ethylbenzene, isopropylbenzene, *n*-propylbenzene
	ARO2	*p*,*m*-xylene, *o*-xylene, 1,3,5-trimethylbenzene, 1,2,4-trimethylbenzene
BVOC	ISOPRENE	Isoprene
	TRP1	α-pinene, camphene, β-pinene, limonene
OVOC	MEOH	methanol
	HCHO	formaldehyde
	CCHO	acetaldehyde
	ACET	acetone
Missing sinks	NO3, HNO3, HONO, HO2, HNO4, HO2H, COOH, ROOH, RNO3, MEK, PROD2, CCO_OOH, RCO_OH, PHEN, HCOOH, RCHO, GLY, MGLY, CRES, BALD, METHACRO, MVK, ISOPROD, DCB1, DCB2, DCB3	
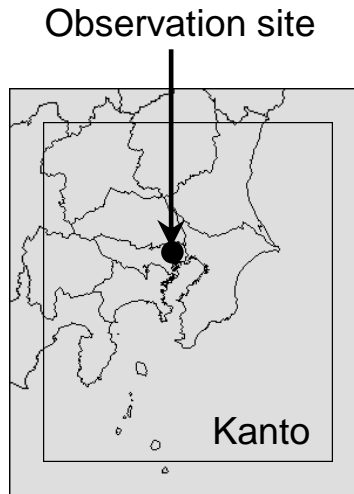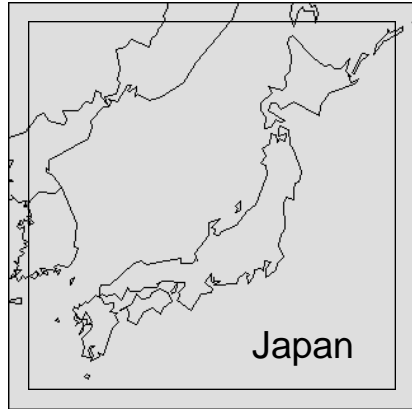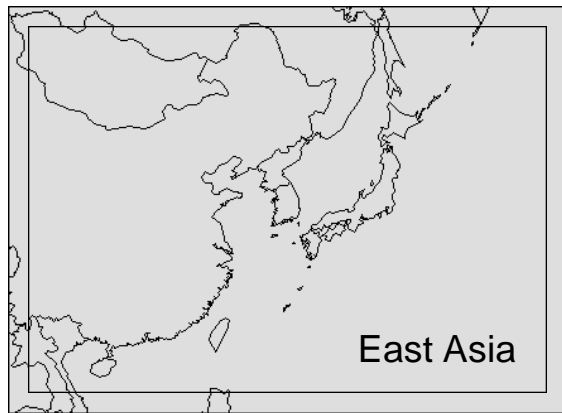
Fig. 1. Target domains of the simulation, with outer lines indicating WRF domains, while inner lines indicating CMAQ domains, and showing the position of the observation site.

Full Screen / Esc

Printer-friendly Version

Interactive Discussion
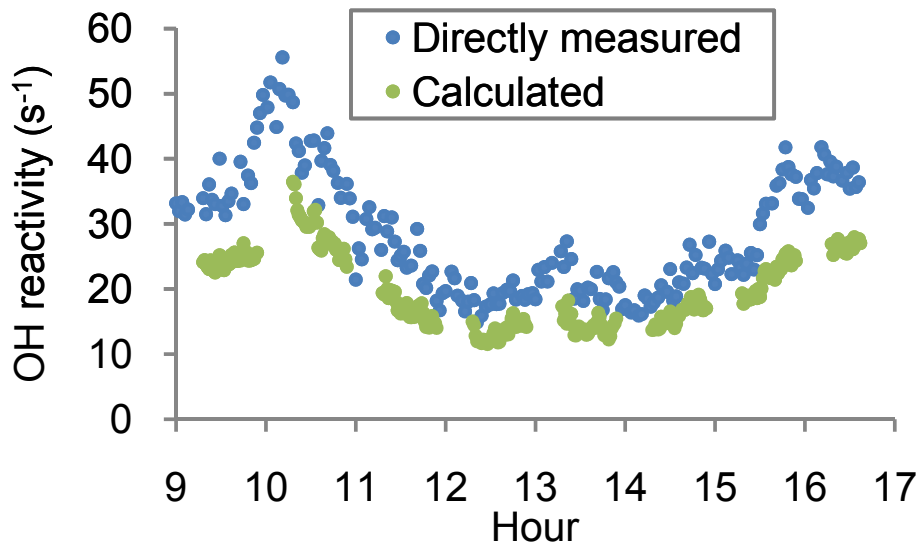
Fig. 2. Directly measured and calculated total OH reactivity, of which calculations are obtained from concentrations and reaction rate coefficients of the measured species on 21 August.
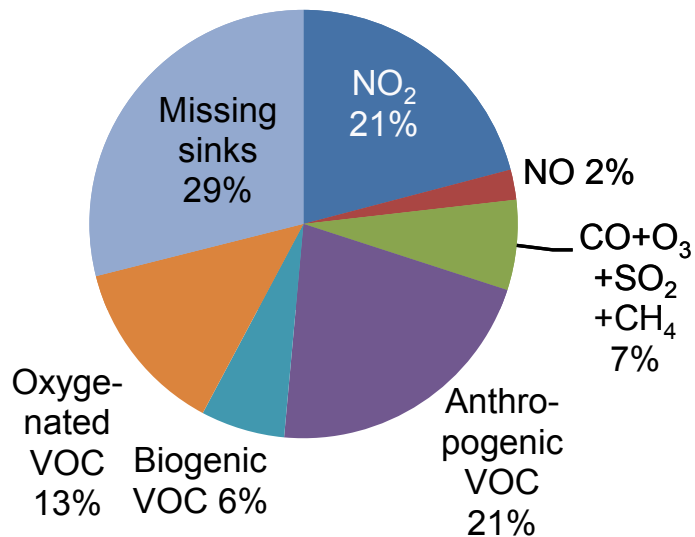
Fig. 3. Contribution of species groups to directly measured OH reactivity which is averaged over the target period.
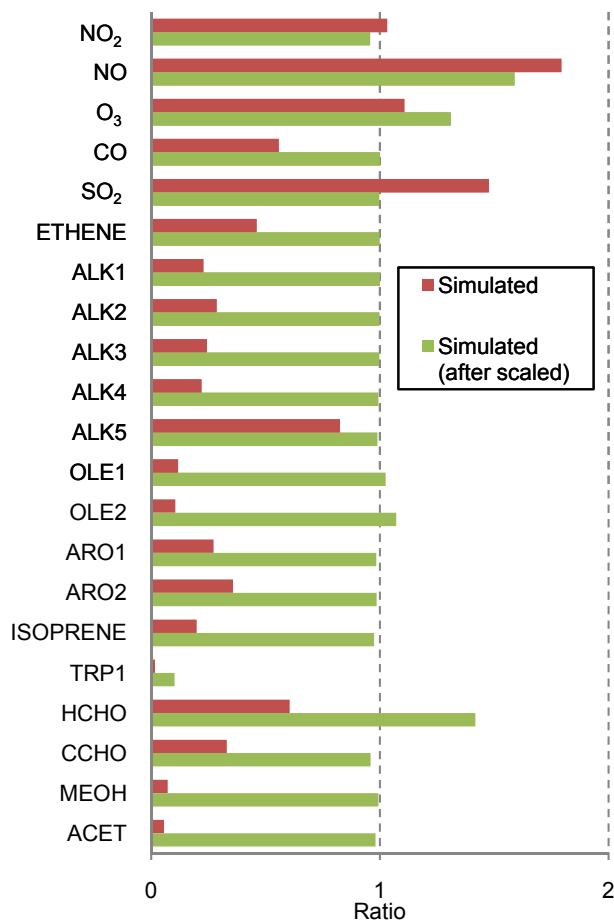
Fig. 4. Ratios of simulated to measured concentrations of SAPRC99 species which are averaged over the target period before and after application of scaling factors.
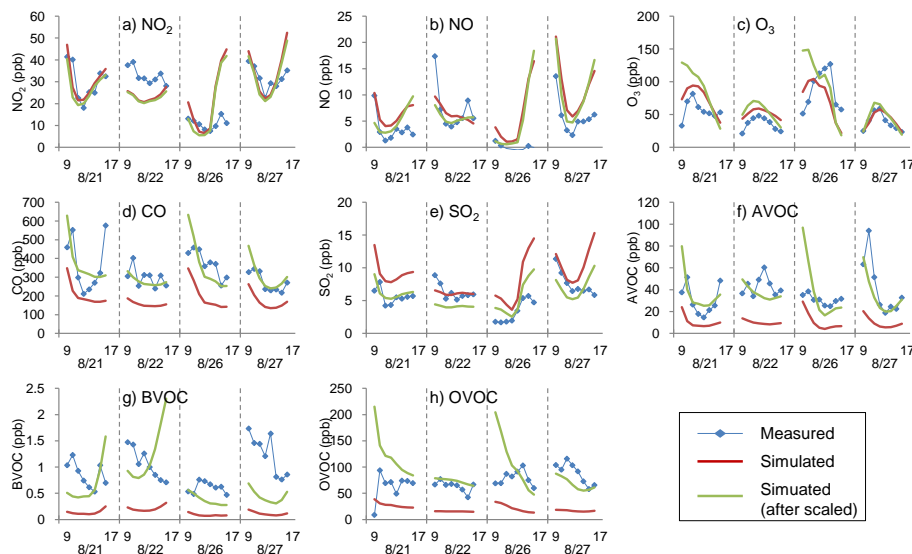
Fig. 5. a–h Time series of measured and simulated concentrations of species groups before and after application of scaling factors.
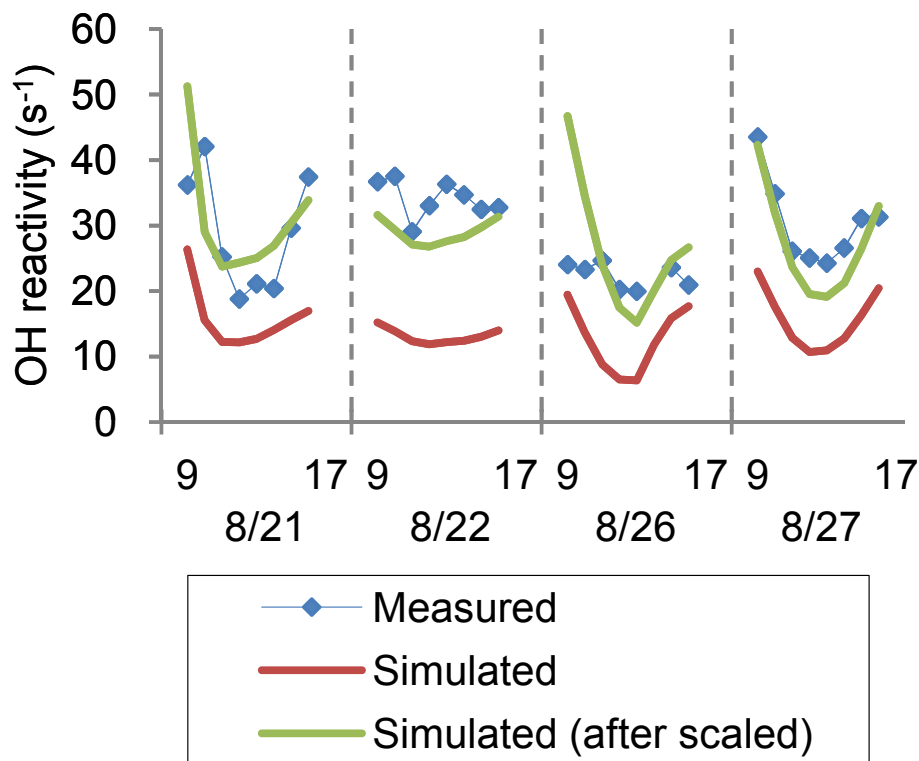
Fig. 6. Time series of measured and simulated total OH reactivity before and after application of scaling factors.

Fig. 7. Measured and simulated OH reactivity of species groups which is averaged over the target period before and after application of scaling factors.
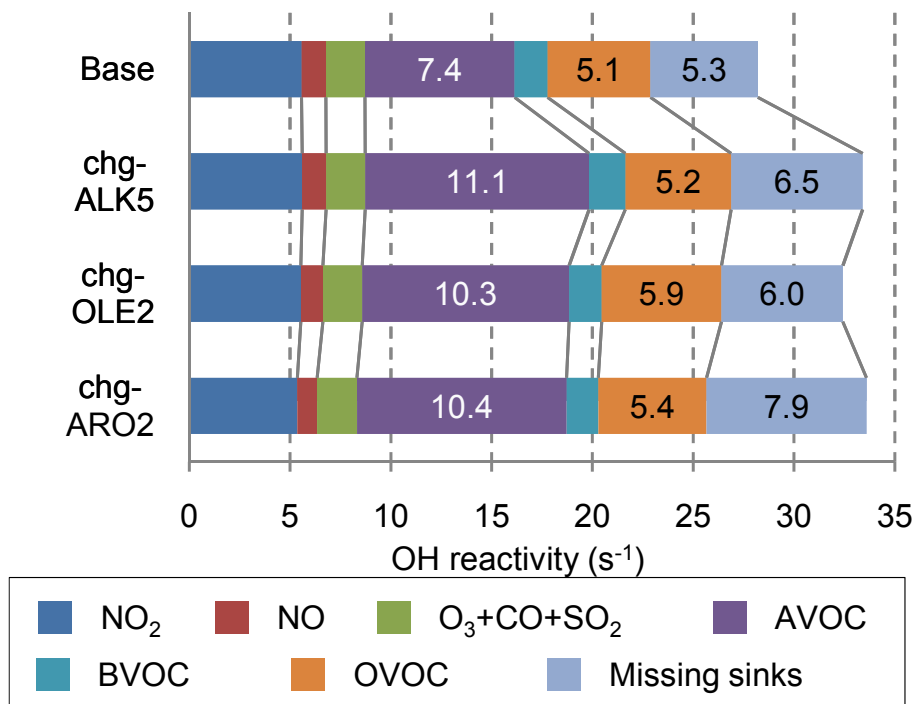
Fig. 8. Contribution of SAPRC species to simulated OH reactivity of missing sinks which is averaged over the target period in the base case.

Full Screen / Esc
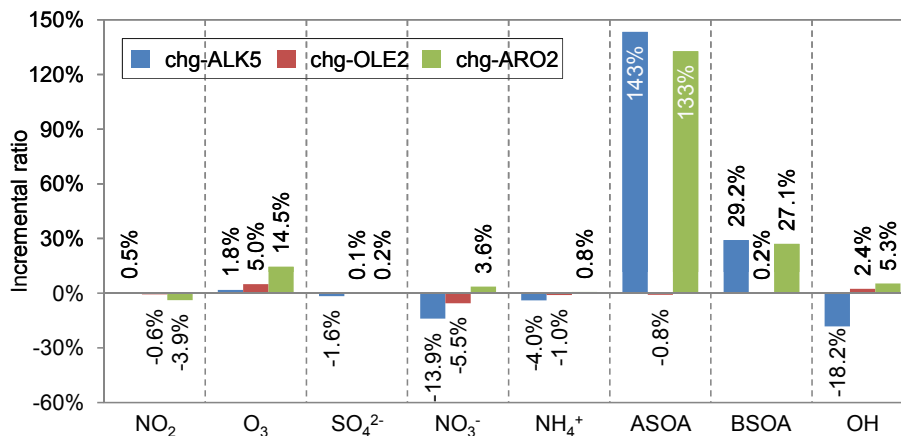
Printer-friendly Version

Interactive Discussion
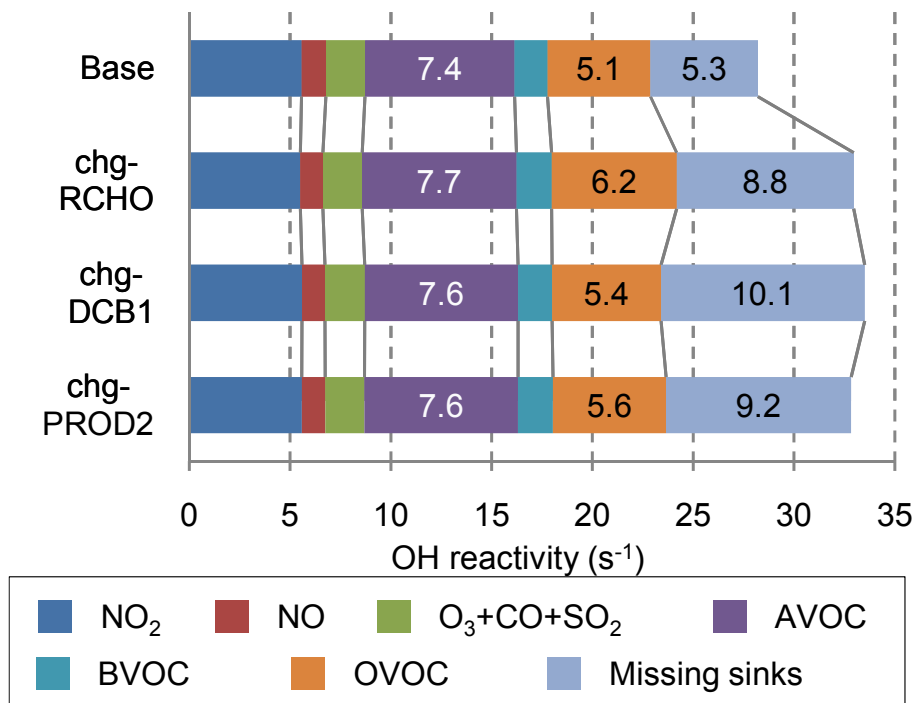
Fig. 9. Simulated OH reactivity of species groups which is averaged over the target period in the base, chg-RCHO, chg-DCB1 and chg-PROD2 cases.
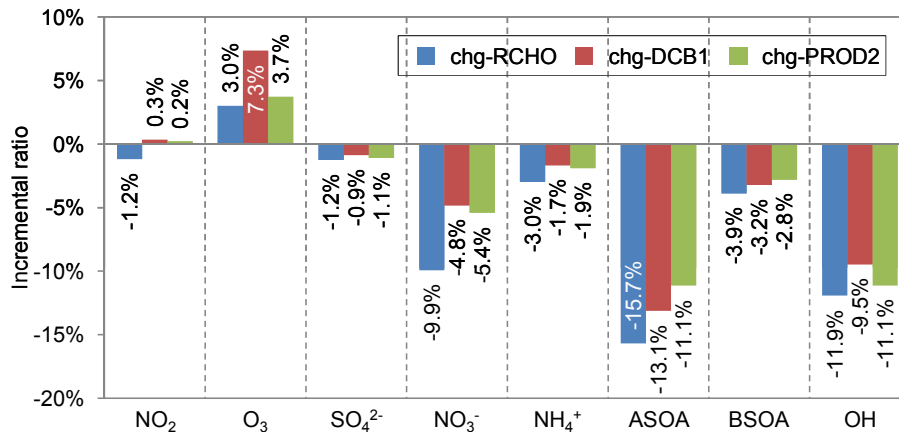
Fig. 10. Incremental ratios of concentrations of NO_2, O_3, OH and secondary aerosol components in the chg-RCHO, chg-DCB1 and chg-PROD2 cases compared to those in the base case, which are averaged over the target period.
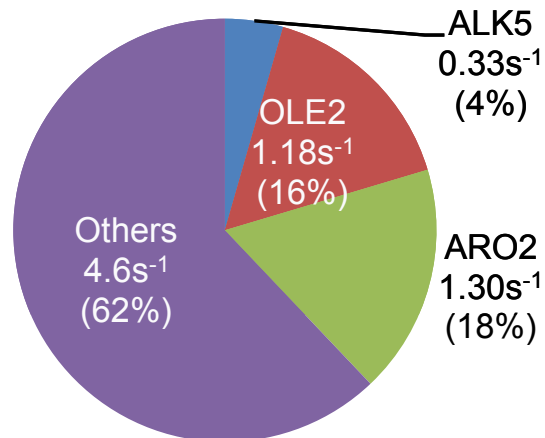
Fig. 11. Contribution of SAPRC species to the simulated OH reactivity of AVOC which is averaged over the target period in the base case.

Fig. 12. Simulated OH reactivity of species groups which is averaged over the target period in the base, chg-ALK5, chg-OLE2 and chg-ARO2 cases.

Fig. 13. Incremental ratios of concentrations of NO_2, O_3, OH and secondary aerosol components in the chg-ALK5, chg-OLE2 and chg-ARO2 cases compared to those in the base case, which are averaged over the target period.